Table S1. *Sequences of oligonucleotide primers used*

Quantitative RT-PCR

*Bcl6*_F	5'-CCTGCAACTGGAAGAAGTATAAG-3'
*Bcl6*_R	5'-AGTATGGAGGCACATCTCTGTAT-3'
*Myc*_F	5'-ATCATCCAGGACTGTATGTGGAG-3'
*Myc*_R	5'-TTCTTGCTCTTCTTCAGAGTCG-3'
*Hprt*_F	5'-GGGGGCTATAAGTTCTTTGC-3'
*Hprt*_R	5'-TCCAACACTTCGAGAGGTCC-3'

Genomic PCR

MycΔ_F:	5'-GCTAGGAAGACTGCGGTGAG-3'
MycΔ_R:	5'-ATTTAAGAGCACCCCCTGCT-3'

Table S2. *Antibodies used for flow cytometry and Western blotting*

A Flow cytometry

Surface antigen	Clone ID	Purchased from
CD19	1D3	BD Biosciences
CD43	S7	BD Biosciences
CD25	7D4	BD Biosciences
CD8	53-6.7	BD Biosciences
IgM (μ-chain)	II/41	BD Biosciences

B Western blot

Antigen	Clone ID	Purchased from
BCL6	D8	Santa Cruz Biotech.
MYC	N-262	Santa Cruz Biotech.
CDKN1B	F-8	Santa Cruz Biotech.
PTEN	A2B1	Santa Cruz Biotech.
ACTB	Polyclonal (ab8227)	Abcam

Table S3. *Retroviral vectors and transduction methods*

Constitutive expression	**Inducible activation**
BCL6-IRES-GFP	BCL6-ER^{T2}
BLNK-IRES-GFP	BLNK-ER^{T2}
Cre-IRES-GFP	Cre-ER^{T2}
IGHμ-IRES-CD8	*Rag2*$^{-/-}$ tTA/μ-chain-tg
None	FoxO1^{CA}-ER^{T2}
BCR-ABL1-IRES-Neo	
MYC-IRES-Puro	
IRES-GFP	
IRES-Neo	
IRES-CD8	
IRES-Puro	

Retroviral transductions

Transfections of the above MSCV-based retroviral constructs encoding BCL6-GFP, MYC-Puro, BLNK-GFP, BCR-ABL1-GFP, Cre-GFP, IGHμ-CD8, BCR-ABL1-IRES-Neo, BCL6-ER^{T2} or Neo, GFP, CD8 and ER^{T2} empty vector controls were performed using Lipofectamine 2000 (Invitrogen, Carlsbad, CA) with Opti-MEM media (Invitrogen). Retroviral supernatant was produced by co-transfecting 293FT cells with the plasmids pHIT60 (gag-pol) and pHIT123 (ecotropic env; kindly provided by Donald B Kohn, UCLA). Cultivation was performed in high glucose Dulbecco's modified Eagle's medium (DMEM, Invitrogen) with GlutaMAX containing 10% fetal bovine serum, 100 IU/ml penicillin, 100 μg/ml streptomycin, 25mM HEPES, 1 mM sodium pyruvate and 0.1 mM non-essential amino acids. Regular media were replaced after 16 hours by growth media containing 10 mM sodium butyrate. After 8 hours incubation, the media was changed back to regular growth media. 24 hours later, the virus supernatant were harvested, filtered through a 0.45 μm filter and loaded by centrifugation (2000 x g, 90 min at 32 °C) two times on 50 ug/ml RetroNectin (Takara, Madison, WI) coated non-tissue 6-well plates. 1-2 x 10^6 pre-B cells were transduced per well by centrifugation at 600 x g for 30 minutes and maintained for 48hrs at 37°C with 5% CO_2 before transferring into culture flasks. Transduction efficiencies were verified by flow cytometry as shown in Figure S1.

Table S4. *Genetic mouse models used in this study*

Mouse strain	Source	Purpose
[a]*BCL6*$^{-/-}$	Riccardo Dalla-Favera, Columbia University	Genetic loss-of-function experiments
[b]*Myc*$^{fl/fl}$	Ignacio Moreno de Alborán, CINES, Madrid, Spain	Inducible deletion of *Myc*
Ighm$^{-/-}$	Jackson Laboratories	Reconstitution of μ-chain expression
[c]*Rag2*$^{-/-}$ tTA/μ -tg	Hans-Martin Jäck, Universität Erlangen	Inducible activation of pre-B cell receptor signaling
[d]*Blnk*$^{-/-}$	Hassan Jumaa, Max-Planck-Institute Freiburg	Reconstitution of Blnk expression
[e]*Pten*$^{fl/fl}$	Hong Wu, UCLA	Inducible deletion of *Pten* (FoxO inactivation)
NOD/SCID	Jackson Laboratories	Transplant recipient mice

Notes:

a Ye BH, Cattoretti G, Shen Q, Zhang J, Hawe N, de Waard R, Leung C, Nouri-Shirazi M, Orazi A, Chaganti RS, Rothman P, Stall AM, Pandolfi PP, Dalla-Favera R. The BCL-6 proto-oncogene controls germinal-centre formation and Th2-type inflammation. Nat Genet. 1997; 16: 161-70.

b de Alboran IM, O'Hagan RC, Gartner F, Malynn B, Davidson L, Rickert R, Rajewsky K. DePinho RA, Alt FW. Analysis of c-Myc function in normal cells via conditional gene-targeted mutation. Immunity. 2001; 14:45-55.

c Hess J, Werner A, Wirth T, Melchers F, Jäck HM, Winkler TH. Induction of pre-B cell proliferation after de novo synthesis of the pre-B cell receptor. Proc Natl Acad Sci U S A. 2001; 98: 1745-50.

d Jumaa H, Wollscheid B, Mitterer M, Wienands J, Reth M, Nielsen PJ. Abnormal development and function of B lymphocytes in mice deficient for the signaling adaptor protein SLP-65. Immunity. 1999; 11: 547-54

e Groszer M, Erickson R, Scripture-Adams DD, Lesche R, Trumpp A, Zack JA, Kornblum HI, Liu X, Wu H. Negative regulation of neural stem/progenitor cell proliferation by the Pten tumor suppressor gene in vivo. *Science*. 2001; 294: 2186-9.

Figure S1. *Verification of transduction efficiencies*

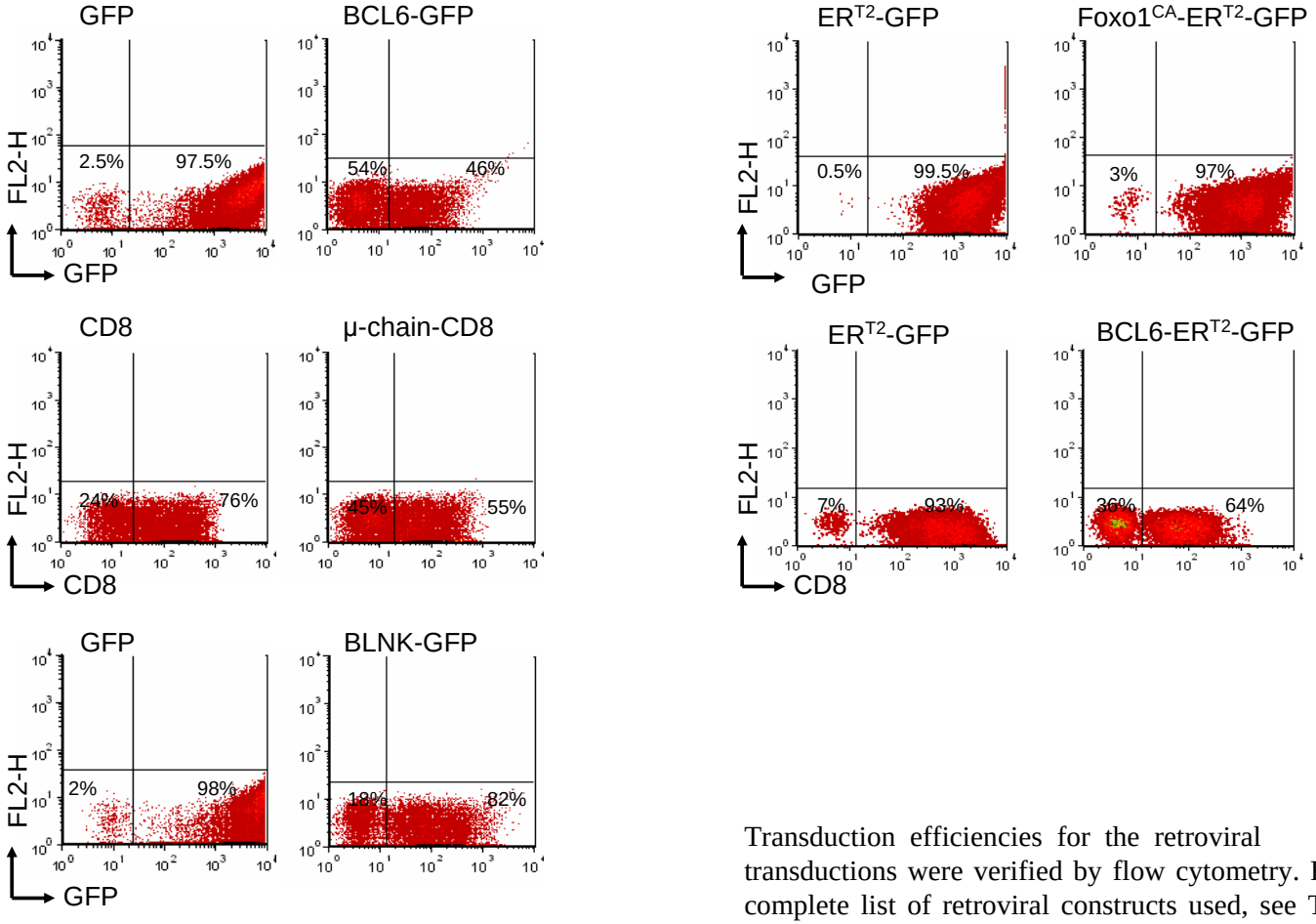

Transduction efficiencies for the retroviral transductions were verified by flow cytometry. For a complete list of retroviral constructs used, see Table S3. In cases where transduction efficiency was lower than 90% (BCL6-GFP, μ-chain-CD8, BLNK-GFP and BCL6-ER^{T2}-GFP), transduced cells and respective empty vector controls were sorted based on expression of either GFP or CD8. For transduction of Ikaros-GFP and FoxO1^{CA}-ER^{T2}-GFP, transduction efficiencies were higher than 90% and no sorts were performed.

Figure S2. *Inducible activation of μ-chain expression initiates pre–BII-cell differentiation*

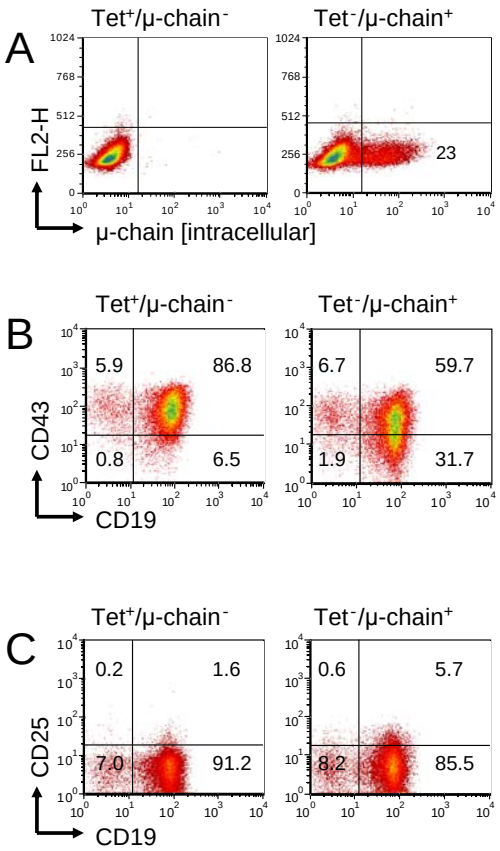

Rag2$^{-/-}$ tTA/μ-chain-transgenic mice[2] are unable to express an endogenous μ-chain because of lack of Rag2-dependent V(D)J recombination. However, the cells carry a functionally pre-rearranged μ-chain under control of tetracycline operator sequences in the germline. In addition, Rag2$^{-/-}$ tTA/μ-chain-transgenic mice express a tetracycline-controlled transactivator (tTA) under control of endogenous transcriptional control elements. Withdrawal of tetracycline results in μ-chain expression (A) and concomitant induction of pre-BII cell differentiation as determined by downregulation of CD43 (B) and upregulation of CD25 (C).

Figure S3. *BCL6 ChIP-on-chip analysis: Recruitment of BCL6 to cell cycle regulating genes in human pre-B ALL*

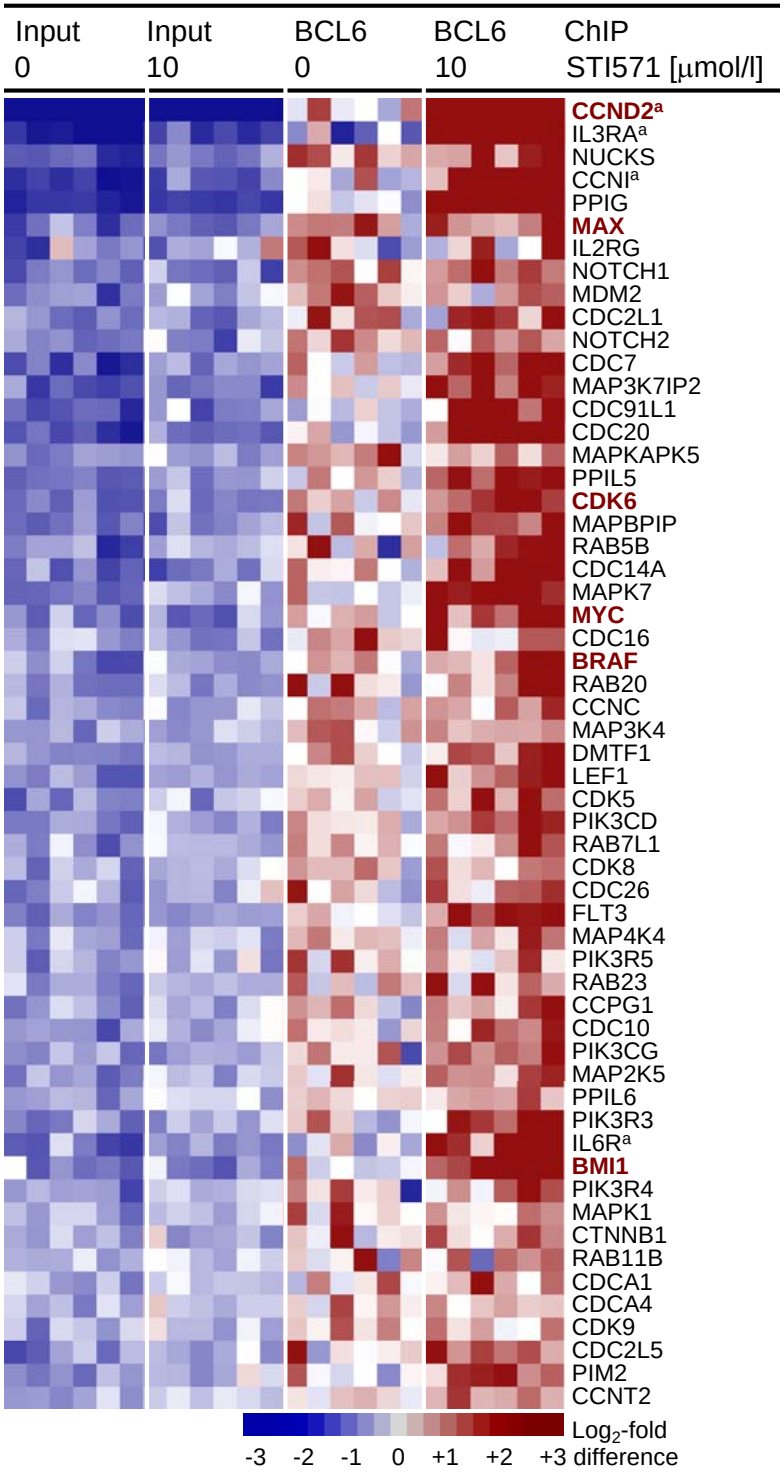

Three *BCR-ABL1*$^{+}$ pre-B ALL cell lines (BV173, Nalm1, Tom1) were treated in the presence or absence of the BCR-ABL1 kinase inhibitor STI571 (10 µmol/l) and subjected to BCL6 ChIP-on-chip analysis together with B cell lymphoma OCI-Ly1 and OCI-Ly7 cell lines. A large number of target genes only show BCL6 recruitment in the presence of Imatinib-treatment. The heatmap depicts a list of genes with a known function in cell cycle progression (e.g. *CCND2* and *MYC*) that are specifically targeted by BCL6. BCL6 target genes with a known function in proliferation of pre-B cells and pre-B cell-derived acute lymphoblastic leukemia are highlighted in red. ChIP-on-chip data are available from GEO under the accession number GSE24404. **Note:** [a]These molecules were identified as BCL6 targets in Duy *et al*., 2011 (Nature 473: 384-388)

ChIP-on-chip protocol and data analysis. BCL6-DNA complexes were immunoprecipitated using an anti-BCL6 polyclonal antibody (N3, Santa Cruz, CA). Enrichment of known target genes was validated by quantitative real time PCR. ChIP products and their respective input genomic fragments were amplified by ligation-mediated PCR as previously reported (Duy et al., 2010). QChIP was performed again at this stage for selected positive control loci to verify that the enrichment ratios were retained. The genomic products of two biological ChIP replicates were labeled with Cy5 (for ChIP products) and Cy3 (for input) and cohybridized on custom-designed genomic tiling arrays generated by NimbleGen Systems Inc. These high-density tiling arrays contain 50-residue oligonucleotides with an average overlap of 25 bases, omitting repetitive elements. Peaks of enrichment for BCL6 relative to input were captured with a five-probe sliding window, and the results were uploaded as custom tracks into the University of California Santa Cruz genome browser and graphically represented as histograms. The cutoff threshold, is defined as 2.5 times the standard deviation above the average relative enrichment on the entire array. Peaks involving five or more oligonucleotide probes above this threshold were considered positive hits.

To identify target genes of BCL6 in these experiments, we compute the log-ratio between the probe intensities of the ChIP product and input and take moving averages of log-ratio of 3 neighboring probes and determine maximum value for each gene promoter and also the random permutation probes as background control. The cut-off for each array is established as higher than 99th percentile of the 24,175 log-ratio values generated from random permutation probes. A locus with maximum moving average above cut-offs in two replicates is considered a potential binding site. Since this high stringent-overlapping approach can produce a high false negative rate, we also computed the correlations among peaks between the replicates as a way to rescue promoters that did not pass cut-off in one replicate. We calculated the Pearson correlation coefficient of the probes signal of the promoter between replicates, and promoters with a correlation higher that 0.8 were rescued and included in our final set of BCL6 targets. In addition, all peaks were mapped back to the genome using BLAT (The BLAST-like Alignment Tool, http://genome.ucsc.edu) to identify genes on opposite strands that could be regulated from the same bidirectional promoter. Two genes were considered to be bidirectional partners when they were located on the opposite strands in a "head-to-head" orientation and their transcription start sites were separated by less than 0.5 kb.

Figure S4. *High levels of Myc expression are required for pre-B ALL cell proliferation*

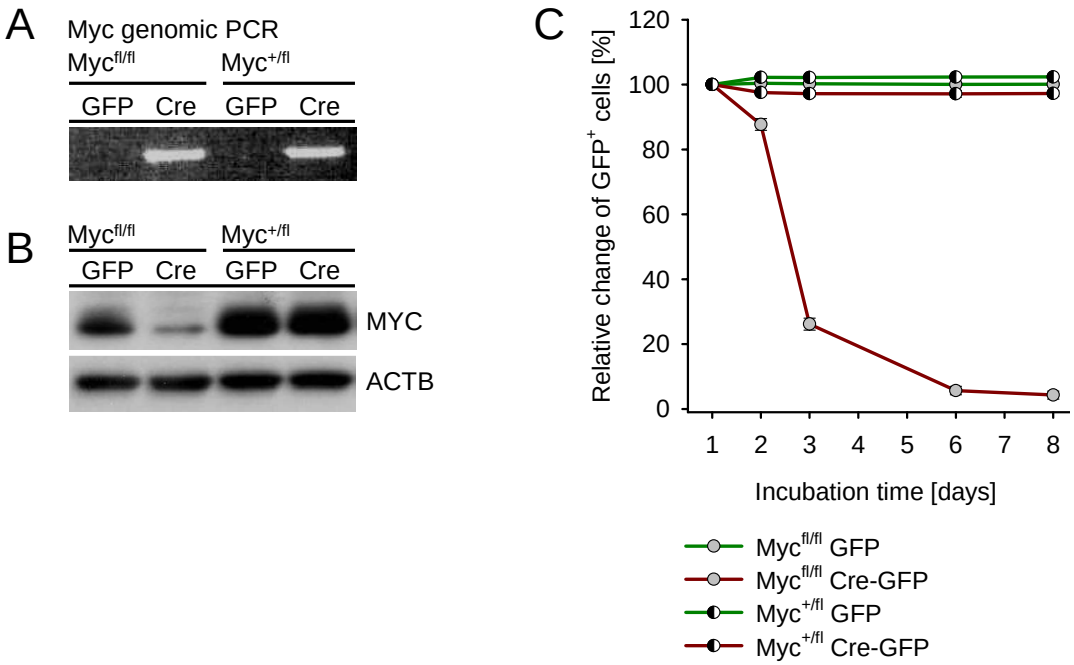

Bone marrow pre-B cells from $Myc^{fl/fl}$ and $Myc^{+/fl}$ mice were transformed with BCR-ABL1 and then transduced with Cre-GFP or a GFP empty vector control. Cre-mediated deletion of floxed Myc alleles was successful as confirmed by genomic PCR (A) and resulted in reduction of Myc protein levels for $Myc^{fl/fl}$ but not $Myc^{+/fl}$ pre-B ALL cells (B). Upon reduction of Myc protein levels in $Myc^{fl/fl}$ pre-B ALL cells, cells rapidly exited cell cycle as measured by reduction of relative percentages of Cre-GFP^+ cells (C). In contrast, $Myc^{+/fl}$ pre-B ALL cells maintained similar Myc protein levels and did not undergo cell cycle arrest.

Figure S5. *Reconstitution of pre-B-cell receptor signaling induces pre-B cell quiescence*

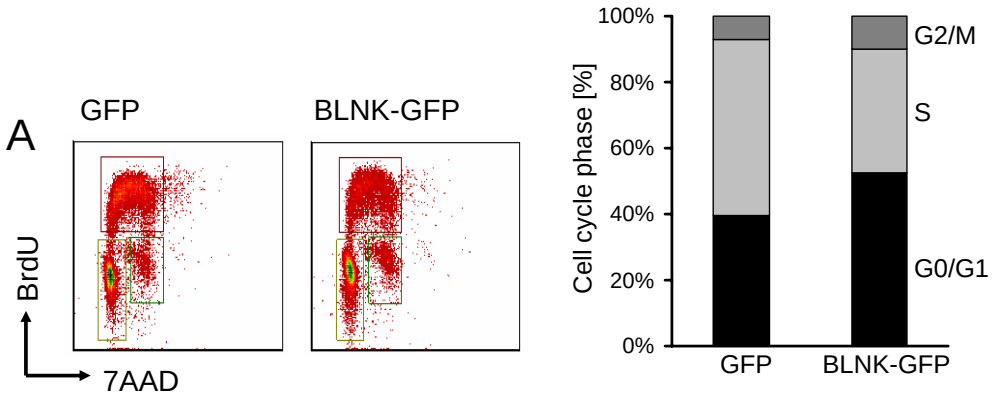

	GFP	BLNK-GFP
G0/1	39.37± 0.5	51.32 ± 4.1
S	53.19 ± 2.7	36.68 ± 1.3
G2/M	6.86 ± 1.3	9.62 ± 2.0

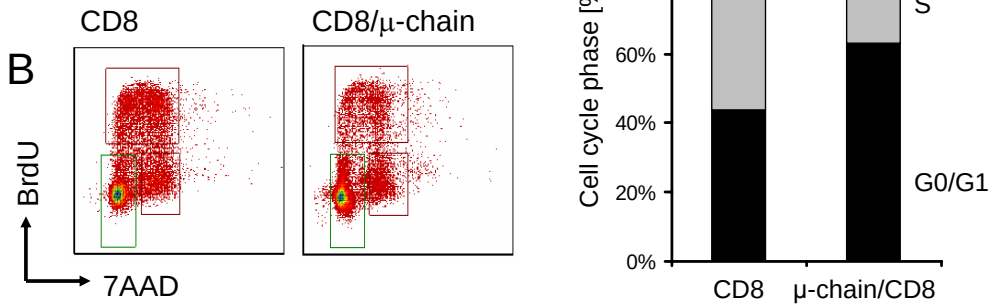

	CD8	CD8/μ-chain
G0/1	40.8 ± 0.5	69.7 ± 9.7
S	37.4 ± 6.5	16.6 ± 7.4
G2/M	18.8 ± 5.3	13.7 ± 1.7

Blnk$^{-/-}$ and *Ighm*$^{-/-}$ BCR-ABL1 ALL cells were reconstituted with retroviral expression of BLNK-GFP (A), CD8/μ-chain (B) or GFP and CD8 empty vector controls. Transduction efficiencies are shown in Fig S1. Three days after transduction, cells were analyzed for their cell cycle profile using BrdU incorporation and flow cytometry. Analysis is done after gating on GFP+ (A) and CD8+ (B) cells. Percentages of cells in G0/G1, S and G2/M phases of the cell cycle are shown - representative of two independent experiments.

Figure S6. *Scenario of BCL6-mediated cell cycle exit downstream of pre-B cell receptor signaling*

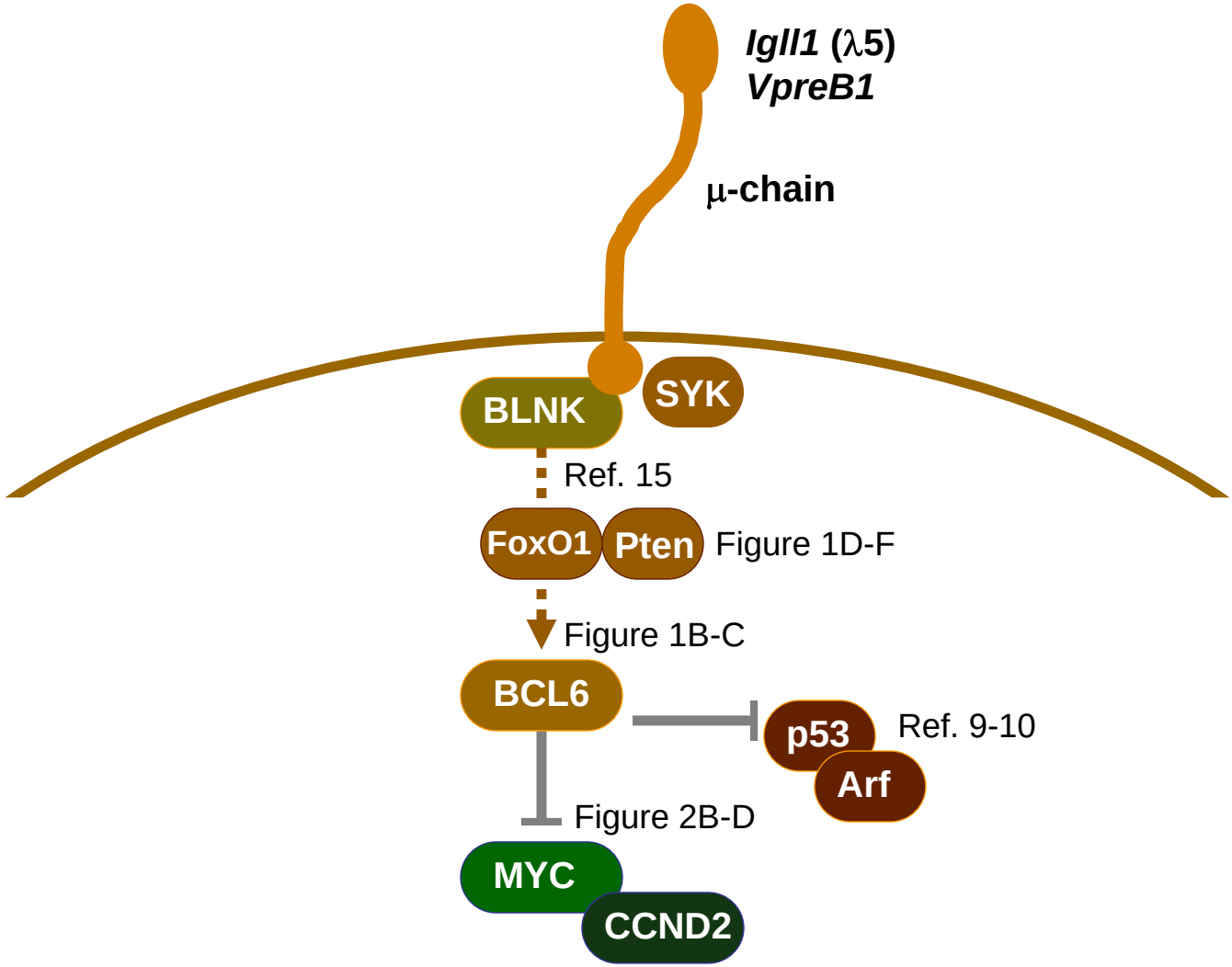

The pre–B-cell receptor upregulates BCL6 via the linker molecule BLNK (see Figure 1B) and Pten-mediated activation of FoxO factors (see Figure 1D-F). BCL6 suppresses *MYC* and *CCND2* causing cellular quiescence (Figure 2B-D). At the same time, BCL6 suppresses p53/Arf, which function as negative regulators of self-renewal and as G0/G1 checkpoint regulators. These findings indicate that cell cycle exit at the transition from large cycling (Fraction C') to the small resting pre-BII (Fraction D) cell stage is mediated by BCL6.